

Hydrogen tunneling in the perovskite ionic conductor $\text{BaCe}_{1-x}\text{Y}_x\text{O}_{3-\delta}$

F. Cordero,¹ F. Craciun,¹ F. Deganello,² V. La Parola,² E. Roncari,³ and A. Sanson³

¹CNR-Istituto dei Sistemi Complessi (ISC), Area della Ricerca di Roma-Tor Vergata, Via del Fosso del Cavaliere 100, I-00133 Roma, Italy

²CNR-Istituto per lo Studio dei Materiali Nanostrutturati (ISMN), Via Ugo La Malfa 153, I-90146 Palermo, Italy

³CNR-Istituto di Scienza e Tecnologia dei Materiali Ceramici (ISTEC), Via Granarolo 64, I-48018 Faenza, Italy

(Received 9 May 2008; revised manuscript received 2 July 2008; published 11 August 2008)

We present low-temperature anelastic and dielectric spectroscopy measurements on the perovskite ionic conductor $\text{BaCe}_{1-x}\text{Y}_x\text{O}_{3-x/2}$ in the protonated, deuterated, and outgassed states. Three main relaxation processes are ascribed to proton migration, reorientation about an Y dopant, and tunneling around the same O atom. An additional relaxation maximum appears only in the dielectric spectrum around 60 K and does not involve H motion but may be of electronic origin, e.g., small polaron hopping. The peak at the lowest temperature, assigned to H tunneling, has been fitted with a relaxation rate presenting crossovers from one-phonon transitions, nearly independent of temperature, to two-phonon processes, varying as T^7 , to Arrhenius type. Substituting H with D lowers the overall rate by eight times. The corresponding peak in the dielectric loss has an intensity nearly 40 times smaller than expected from the classical reorientation of the electric dipole associated with the OH complex. This fact is discussed in terms of coherent tunneling states of H in a cubic and orthorhombically distorted lattice, possibly indicating that only H in the symmetric regions of twin boundaries exhibit tunneling, and in terms of reduction in the effective dipole due to lattice polarization.

DOI: [10.1103/PhysRevB.78.054108](https://doi.org/10.1103/PhysRevB.78.054108)

PACS number(s): 77.22.Gm, 66.35.+a, 62.40.+i

I. INTRODUCTION

Perovskite cerates and zirconates are a class of materials that, with appropriate doping, exhibit ionic conductivities of both O vacancies and protons and therefore are suitable as solid electrolytes for fuel cells, gas sensors, and other electrochemical devices. Dissolution of H is achieved in two steps:¹ The material is doped with lower valence cations, e.g., $\text{BaCe}_{1-x}\text{Y}_x\text{O}_{3-x/2}$ (BCY), where the partial substitution of Ce^{4+} with Y^{3+} introduces charge-compensating O vacancies. The material is then exposed to a humid atmosphere at high temperature, so that the H_2O molecules may dissociate, each of them filling an O vacancy and contributing with two H atoms. Infrared spectroscopy² and diffraction³ experiments indicate that H is bound to an O, forming a OH^- ion, but also makes some hydrogen bonding with a next-nearest O atom. The proton diffusion is believed to consist of a rapid rotation about the O atom to which it is associated and slower jumps to one of the eight next-nearest-neighbor O atoms, with which an instantaneous hydrogen bond is established [see Fig. 7(a)]. It has also been proposed, however, that in some distorted zirconates and titanates the rotational barrier may be higher than the transfer barrier.⁴ In various cubic perovskites ABO_3 , there are four equilibrium orientations of the OH^- complex, with an OH separation of 0.9–1.0 Å and H pointing in the $\langle 100 \rangle$ directions perpendicular to the B-O-B bond.^{5,6} In the presence of dopants or noncubic distortions, such positions would be shifted.³ It is very likely that the fast local motion of H about the same O is dominated by tunneling. However so far no quantitative measurements of the associated correlation times have appeared except for quasielastic-neutron-scattering experiments on hydrated $\text{Ba}(\text{Ca}_{0.39}\text{Nb}_{0.61})\text{O}_{2.91}$, where a fast local motion has been detected above room temperature with an apparent activation energy of ~ 0.1 eV.⁷ Also in $\text{SrCe}_{0.95}\text{Yb}_{0.05}\text{O}_{2.97}$ a broad

quasielastic component has been attributed to fast proton rotation,⁸ but no reliable measurement of the associated rate was possible.

There is a controversy on the effect of dopants on the proton mobility, as reviewed in Ref. 9: On one hand there are several indications for trapping,^{9–12} with formation of stable dopant-H complexes. However it has also been proposed that the excess doped charge distributes over all O sites, causing an increase in the hopping barrier for the proton over the whole lattice.¹³

Anelastic and dielectric spectroscopies may contribute to answering such issues, since both an electric and an elastic dipole are associated with a OH^- ion or an Y-OH^- complex. Moreover each type of jump or reorientation with characteristic time $\tau(T)$ causes a maximum of the losses at the temperature T and frequency $\omega/2\pi$ such that $\omega\tau(T) \approx 1$. Anelastic relaxation is particularly useful, since it is almost insensitive to electronic conduction and is not affected by charged interface layers. We present anelastic and dielectric spectroscopy measurements on protonated, deuterated, and outgassed $\text{BaCe}_{1-x}\text{Y}_x\text{O}_{3-x/2}$, where different relaxation processes are ascribed to H migration, reorientation about an Y dopant, and tunneling about the same O atom. The focus will be on the last type of motion.

II. EXPERIMENT

The starting powders of BCY were prepared by autocombustion synthesis, which is an easy and convenient solution-based method for the preparation of nanometric mixed oxide powders. The method¹⁴ is an improvement of that for metal citrates described in the literature.¹⁵ Stoichiometric amounts of highly purified metal nitrates were dissolved in distilled water and mixed with citric acid, which acted both as metal ion complexant and as fuel. The citric acid to metal nitrate

ratio was maintained at 2. Ammonium nitrate was added to regulate the fuel to oxidant ratio (citric acid/total nitrate ion ratio) to 0.4 and ammonia solution (30 % wt) was added to regulate the pH value to 6. The water solution was left to evaporate at 80 °C under constant stirring in a beaker immersed in a heated oil bath until a whitish and sticky gel was obtained. The temperature was then raised to 200 °C until the gel became completely black and dry. The beaker was then put directly on the hot plate at 250–300 °C until the autocombustion reaction occurred, leaving the powdered product. Crystallization was completed by firing the combusted powders in stagnant air at 1000 °C for 5 h. No weight loss occurred during the synthesis and no oxide segregation has been detected by x-ray diffraction, so that we assumed the nominal compositions $\text{BaCe}_{1-x}\text{Y}_x\text{O}_{3-x/2}$ with $x=0.1$ (BCY10) and $x=0.15$ (BCY15). The nanopowders were first uniaxially pressed at 50 MPa and then isostatically pressed at 200 MPa, obtaining $60 \times 7 \times 6 \text{ mm}^3$ bars, which were sintered at 1500 °C for 10 h. The bars were cut as thin reeds about 4 cm long and 1 mm thick, whose major faces were covered with Ag paint.

The maximum molar concentration $c_{\text{H/D}}$ of H and D was measured from the change in weight when the sample state was changed between fully outgassed (up to 730 °C in vacuum of $<10^{-5}$ mbar) and hydrated for 1–2 h at 520 °C in a static atmosphere of 50–100 mbar H_2O or D_2O followed by slow cooling. It was found that $c_{\text{H}}=0.14$ for $x=0.15$ and $c_{\text{H}} \leq 0.086$ for $x=0.10$, slightly less than the theoretical maximum $c_{\text{H}}=x$.

The elastic compliance $s(\omega, T) = s' - is''$ was measured by electrostatically exciting the flexural modes of the bars suspended in vacuum on thin thermocouple wires in correspondence with the nodal lines. The first, third, and fifth modes could be measured, whose frequencies are in the ratio of 1:5.4:13.3, the fundamental frequencies of samples being $\omega/2\pi \approx 2.8 \text{ kHz}$. The elastic-energy-loss coefficient, or the reciprocal of the mechanical quality factor,¹⁶ $Q^{-1}(\omega, T) = s''/s'$, was measured from the decay of the free oscillations or from the width of the resonance peak. The elastic compliance s is the mechanical analog of the dielectric susceptibility χ , with Q^{-1} corresponding to $\tan \delta$.

The dielectric permittivity $\varepsilon = \varepsilon' - i\varepsilon''$ was measured with a HP 4284A impedance bridge with a four wire probe between 3 and 100 kHz in the same cryostat used for the anelastic measurements. After depositing the Ag electrodes, an intense dielectric relaxation process, identified with the motion of charge carriers within a Schottky barrier at the electrode interface, completely masks the true bulk relaxation. Such an effect was suppressed by applying 40 V up to $\sim 500 \text{ K}$, switching the direction of the dc current in order to avoid electromigration of O vacancies or protons.¹⁷

A defect hopping or reorienting with characteristic time τ and causing changes $\Delta\lambda$ in its elastic quadrupole and Δp in its electric dipole contributes with a Debye peak to the imaginary parts of the elastic compliance s and dielectric permittivity ε as¹⁸

$$s'' = \frac{c(\Delta\lambda)^2}{3v_0k_B T \cosh^2(E/2T)} \frac{\omega\tau}{1 + (\omega\tau)^2} \quad (1)$$

and

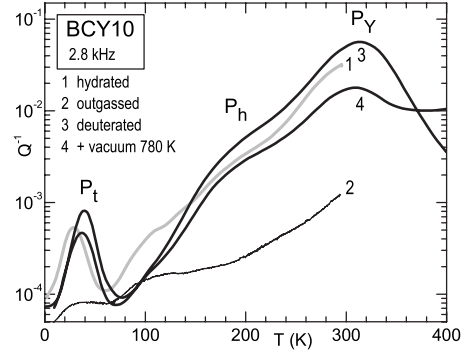


FIG. 1. Anelastic spectra of BCY10 measured in different conditions of hydration with H_2O and D_2O .

$$\varepsilon'' = \frac{c(\Delta p)^2}{3\varepsilon_0 v_0 k_B T \cosh^2(E/2T)} \frac{\omega\tau}{1 + (\omega\tau)^2}, \quad (2)$$

where c is the molar concentration of relaxing defects, v_0 is the molecular volume, and E is the energy difference between the states participating in relaxation. When $E \geq T$, the higher-energy state becomes less populated. Therefore there is a reduced change in the defect populations under application of the probe field with respect to the case $E=0$. The consequent reduction in the relaxation strength is described by the factor $\text{sech}^2(E/2T)$.¹⁹

III. RESULTS

A. Anelastic spectra

Figure 1 presents the anelastic spectra of $\text{BaCe}_{0.9}\text{Y}_{0.1}\text{O}_{3-\delta}$ measured at the fundamental frequency of 2.8 kHz: (1) in the as prepared state, therefore nearly saturated with H_2O ; (2) after outgassing H_2O at 900 °C in a flux of pure O_2 for 2.5 h; (3) after keeping in a static atmosphere of $\sim 70 \text{ mbar}$ D_2O at 520 °C followed by cooling at 1 °C/min; and (4) after having measured in vacuum up to 500 °C with partial loss of D_2O .

There are at least three relaxation processes clearly due to the presence of H or D: the peak labeled P_Y at $\sim 300 \text{ K}$, P_h at $\sim 200 \text{ K}$, and P_t at $\sim 30 \text{ K}$. Above 400 K the contributions due to O vacancies start. All these peaks shift to higher temperature when measured at higher frequency. A preliminary analysis yields activation energies of 0.58 eV with $\tau_0 \sim 3 \times 10^{-14} \text{ s}$ for P_Y and $\sim 0.4 \text{ eV}$ for P_h ; the latter is likely composed of different processes. These peaks are quite broader than pure Debye relaxations and the possible difference in relaxation parameters between H and D is not apparent without an accurate analysis. They must be due to hopping of H between different O atoms. Peak P_t is the focus of the present work. It shifts from 29 to 38 K when H is replaced with D, clearly indicating that it is due to the fast motion of H around the same O atom with a dynamics dominated by tunneling. An additional peak at $\sim 100 \text{ K}$ might also be due to H and it possibly shifts to higher temperature after substitution of H with D. However its nature is not as clear as for the other processes and we will not discuss it further.

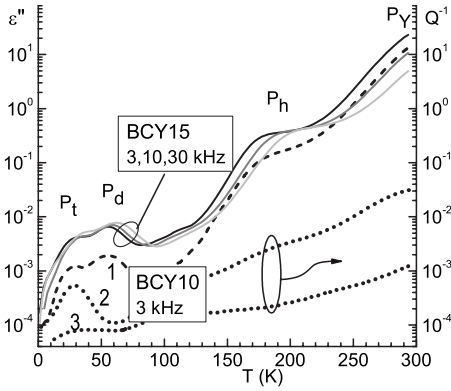


FIG. 2. Dielectric (left-hand scale) and anelastic (right-hand scale) spectra of BCY: ϵ'' of hydrated BCY15 at 3, 10, and 30 kHz (continuous lines) and ϵ'' of hydrated BCY10 at 3 kHz (curve 1). The dotted lines are Q^{-1} of hydrated (curve 2) and outgassed (curve 3) BCY10 measured at 2.8 kHz.

B. Comparison between anelastic and dielectric spectra

All the peaks appearing in the anelastic spectrum are present also in the dielectric one, which also displays an additional maximum P_d at ~ 60 K. Figure 2 shows ϵ'' of hydrated BCY15 and BCY10 ($c_H=0.078$; curve 1). The latter is compared with the elastic counterpart Q^{-1} in the hydrated (curve 2) and outgassed (curve 3) states, measured at the same frequency of 3 kHz. It appears that the intensities of peaks P_t , P_h , and P_Y span more than 4 orders of magnitude in ϵ'' but only 2 in Q^{-1} , meaning that the fast tunneling motion of H produces a much smaller change in the electric dipole than in the elastic dipole, compared to the hopping motion. On the other hand, the peak temperatures and activation energies appear to be practically the same in the dielectric and anelastic losses. These dielectric measurements on BCY15 have been made after full elimination of the charge relaxation at the electrodes, so that the intensities of P_Y and P_h are reliable. Figure 3 shows ϵ'' of both hydrated (thick lines) and deuterated (thin lines) BCY15. While peak

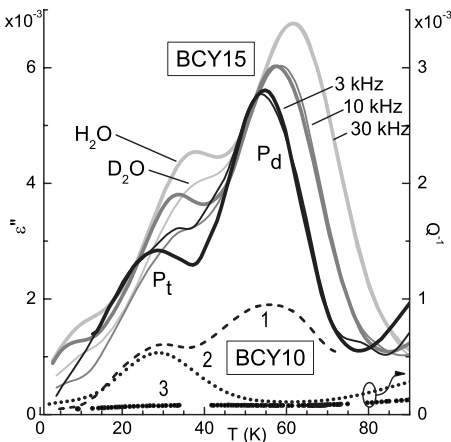


FIG. 3. Low-temperature region of the dielectric and anelastic spectra of BCY in Fig. 2. The ϵ'' (left) and Q^{-1} (right) scales are chosen in order to emphasize the near coincidence of dielectric and anelastic P_t (curves 1 and 2).

P_t shifts to higher temperature after the isotope substitution of H with D as for the anelastic case, peak P_d remains completely unaffected. This fact, together with its absence in the anelastic losses, indicate that P_d is not connected with the H motion but is likely of electronic origin. Curves 1–3 in Fig. 3 are the same dielectric and anelastic curves of BCY10 appearing in Fig. 2, but this time the two scales are chosen in order to yield the same intensity of P_t . Unfortunately, experimental difficulties connected with the elimination of the metal-semiconductor barrier at the electrodes did not allow us to obtain significant dielectric spectra in the outgassed state, so that it is possible to determine that the intensity of P_d almost triplicates in the hydrated state passing from 10% to 15%Y doping, but nothing can be said on its dependence on the content of H or O vacancies.

IV. DISCUSSION

A. Proton hopping and trapping

In what follows we will identify peak P_Y with hopping of H among the O atoms of YO_6 octahedra, namely, with the reorientation of the Y-H complex, and P_h with hopping over CeO_6 octahedra, with the possible contribution of the formation/dissociation of Y-H complexes. These assignments are suggested by the fact that it is natural to assume that $(OH)^-$ ions, having a formal charge of +1 with respect to O^{2-} , may form relatively stable complexes with trivalent dopants Y^{3+} , having a formal charge of -1 with respect to Ce^{4+} . Then, P_Y with higher intensity and activation energy should be due to the more numerous H atoms associated with Y, while P_h should be due to the faster jumps of the less numerous H atoms not associated with Y. The assignment of anelastic relaxation peaks to dopant-H complexes has already been proposed for $BaCe_{1-x}Nd_xO_{3-\delta}$ (Ref. 20) and $(Ba, Sr)Ce_{1-x}Yb_xO_3$,²¹ although the argument that the $(OH)^-$ ion has the same symmetry as the crystal and therefore cannot produce anelastic relaxation unless forming defect complexes²⁰ is incorrect. Additional experimental indications that H is trapped by trivalent dopants in $BaCe_{1-x}Y_xO_3$ are the analysis in terms of two components of the quasielastic-neutron-scattering peak¹⁰ and the observation with extended x-ray-absorption fine structure (EXAFS) of an enhancement of the disorder in the environment of Y after hydration.¹² Also first-principles calculations and Monte Carlo simulations of the proton diffusion indicate that dopants act as traps.^{9,22}

On the other hand, there are also experiments suggesting the absence of significant trapping, such as an NMR investigation¹³ on $BaCe_{1-x}Y_xO_3$ with $x=0.01$ and 0.1, where the correlation time deduced from the 1H NMR relaxation is the same at both doping levels and reproduces the conductivity with a simple hopping model without trapping. At this stage, it cannot be completely excluded from our data that there is indeed very little trapping effect from Y dopants, and the two main anelastic relaxation processes P_Y and P_h are associated with H hopping among O1 and O2 atoms of the orthorhombic structure, having different symmetries. It is possible that H binds to O1 and to O2 with different probabilities, as neutron-diffraction experiments and molecular-

dynamics simulations suggest,^{3,23} and it jumps within the respective sublattices with different rates, thus giving rise to peaks with distinct intensities and temperatures. In the discussion we will also mention the possibility that in the distorted orthorhombic structure the reorientation of the OH ions is much slower than found in the higher-temperature phases, and P_h is due to such slow reorientation.

B. Fit of the anelastic P_i

The relaxation modes of the fast reorientation of OH among four positions can be found by solving the rate equations for classical hopping between the four H sites or the quantum-mechanical problem with tunneling between nearest-neighbor orientations. In the classical symmetric case, there are two modes: one active in the dielectric relaxation and another in the anelastic relaxation, with a rate twice larger. In the case that the site energies are different, however, the modes become three, all contributing to both anelastic and dielectric relaxations, and with possibly widely changing rates, depending on the type of asymmetry and the degree of coherence of the eigenstates of H plus polaronlike distortion of the surrounding atoms. At variance with the geometrically analogous case of the reorientation of Zr-H complexes in Nb,²⁴⁻²⁷ in highly doped and orthorhombic BCY it is not possible to distinguish different peaks arising from these modes. Therefore we will limit ourselves to fit P_i with a single relaxation time τ plus broadening, as

$$Q^{-1}(\omega, T) = \frac{\Delta_0}{T \cosh^2(E/2k_B T)} \frac{\sqrt{\alpha\beta}}{(\omega\tau)^\alpha + (\omega\tau)^{-\beta}}, \quad (3)$$

where the parameters $\alpha, \beta \leq 1$ produce broadening of the low- and high-temperature sides of the peak, respectively. When $\alpha = \beta = 1$ the above expression reduces to a Debye peak. The parameter E is the energy difference between the configurations involved in relaxation and must be introduced in order to reproduce the enhancement of the peak height at higher frequency.¹⁹ The relaxation rate was modeled as

$$\tau^{-1} = \tau_{1\text{ph}}^{-1} \coth(E/2k_B T) + (T/T_{2\text{ph}})^n + \tau_0^{-1} \exp(-W/T). \quad (4)$$

Such an expression is similar to that used by Kuskovsky *et al.*²⁸ for the low-temperature dielectric relaxation in $\text{Ba}_{1-x}\text{Nd}_x\text{CeO}_{3-x/2}$. It does not rely on a model of the interaction between a precise defect geometry and the actual phonon bath, but it is able to describe the main hopping regimes, including tunneling in an insulating crystal. One expects that, starting from low temperature, the transitions between the defect eigenstates occur through processes involving one phonon, then two phonons, and finally several phonons or semiclassical hopping.²⁷ In the one-phonon regime the transition rate is $\tau_{1\text{ph}}^{-1} \coth(E/2k_B T)$, which becomes temperature independent when $k_B T$ is smaller than the separation E between the eigenstates. The latter has a form of the type $E \approx \sqrt{t^2 + a^2}$, where the tunneling matrix element t is expected to be smaller than the typical energy asymmetry a between the site energies due to the orthorhombic distortion and disordered nature of the BCY solid solution. In the fit $E = a$. The two-phonon relaxation rate approximately depends on temperature through a power law,²⁹⁻³¹ with $5 \leq n \leq 9$, depending

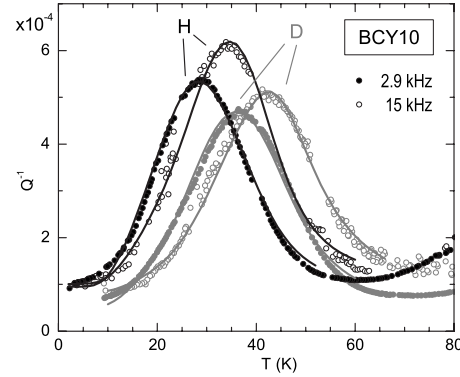


FIG. 4. Fit of the anelastic P_i of hydrated and deuterated BCY10, measured at 2.9 and 15 kHz.

on the type of interaction with acoustic phonons and on the energy difference between H sites. For interaction with optical phonons of frequency ω_0 , an Arrhenius-type $\exp(-\hbar\omega_0/k_B T)$ dependence is predicted.³⁰ At sufficiently high temperatures an Arrhenius-type temperature dependence is always found, although the pre-exponential term τ_0 is not necessarily related to the frequency of a local H vibration mode but depends also on the overlap of the wave functions of H in adjacent sites. In addition the barrier W may contain significant corrections due to phonon fluctuations with respect to the static potential.

We found that all the three contributions to τ^{-1} are necessary to obtain a good fit: The one-phonon term reproduces the low-temperature broadening of P_i without resorting to extremely small values of α . The introduction of the power law significantly improves the fit quality around the maximum. The Arrhenius contribution is not essential to obtain good fits, since its suppression can be partially compensated for by an increase in β , namely, by diminishing the broadening at high temperature. However, if one wants to keep $\alpha \approx \beta$ the Arrhenius contribution must be included. The condition $\alpha \approx \beta$ appears desirable if such parameters should describe the broadening of a Debye peak due to lattice disorder and not to other types of interactions, such as collective interactions among H atoms.

The continuous lines in Fig. 4 are fits of anelastic P_i of BCY10 both hydrated and deuterated with the above expressions plus a linear background. In view of the partial duplication of the effects of some parameters, such as the high-temperature broadening β and the Arrhenius τ_0 and W , these fits are not unique. We tried to obtain a physically sound combination of the parameters. The mean asymmetry energy is determined quite precisely as $E/k_B = 64$ K from the temperature dependence of the peak intensities. Regarding broadening, it is possible to obtain good fits with $\alpha = \beta = 0.5$ for both H and D, although $\beta = 0.38$ for H gives a slightly better interpolation, as in Fig. 4. These values of α and β imply a broadening that is conspicuous but expected, in view of the high lattice disorder. The other parameters are $\tau_0 = 7.7 \times 10^{-14}$ s (1.1×10^{-13} s), $W = 744$ K (820 K), $T_{2\text{ph}} = 6.7$ K (8.4 K), $n = 7$, and $\tau_{1\text{ph}}^{-1} = 7300$ s⁻¹ (990 s) for H (D). The resulting $\tau_{\text{H,D}}^{-1}(T)$ are plotted in Fig. 5 and it turns out that $\tau_{\text{H}}^{-1}/\tau_{\text{D}}^{-1} \approx 8$ at all temperatures. Such a ratio certainly

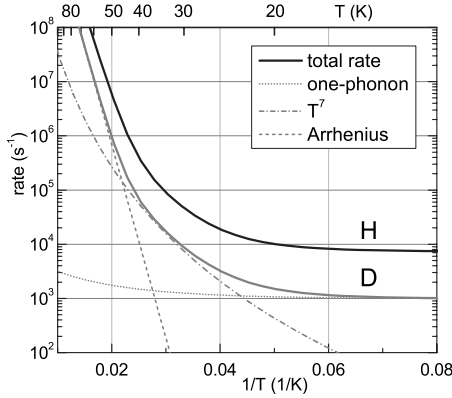


FIG. 5. Relaxation rates τ^{-1} used in the fits in Fig. 4. The rate for deuterium is decomposed into one- and two-phonon and Arrhenius-type contributions.

indicates a nonclassical effect of the isotope mass on the H dynamics. The barrier $W \approx 800$ K of the Arrhenius-type contribution is close to the activation energy for rotational diffusion obtained from quantum-molecular-dynamics simulations^{23,32} and to that extracted from quasielastic neutron scattering in $\text{Ba}(\text{Ca}_{0.39}\text{Nb}_{0.61})\text{O}_{2.91}$.⁷ It cannot be excluded, however, that it rather originates from two-phonon interaction with optical phonons,³⁰ considering that the infrared absorption bands in various cerates range from $\hbar\omega/k_B = 600$ to 1000 K ($400\text{--}700$ cm^{-1}).³³ The power law with $n = 7$ instead is typical of two-phonon transitions of asymmetric states interacting with acoustic phonons. Lower values of n yield definitely worse fits, while $n \approx 7.8$ is found if the Arrhenius contribution is omitted.

C. Fit of dielectric P_t and P_d

The most reliable fit is for BCY10, where peak P_d has a reduced intensity. Below 100 K, $\varepsilon'(\omega, T)$ has already approached the limiting high-frequency value $\varepsilon_\infty = 20.1$, so that the $\varepsilon''(T) = \varepsilon_\infty \tan\delta(T)$. In Fig. 6 we show $\tan\delta$ at 10 , 30 , and 100 kHz; at lower frequency the noise was too large to add significant information. Note that, due to the imperfect compensation of the cables' impedance at low temperature and the very small values of the dielectric losses, the $\tan\delta$ curves can be arbitrarily shifted in the ordinate scale. In fact, it was verified by switching on and off the cable compensation that

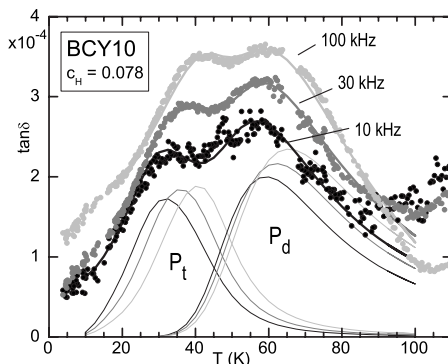


FIG. 6. Fit of the dielectric spectrum of BCY10.

below 150 K such a correction became independent of temperature and therefore introduced only a shift of the $\tan\delta$ curves.

The shapes and temperatures of dielectric and anelastic P_t need not be identical, since the various relaxation modes contributing to them may have different strengths for anelastic and dielectric relaxations. Yet, we chose not to let all the parameters of P_t vary freely, due to the still overwhelming presence of P_d at higher temperature and possibly to the presence of another relaxation at lower temperature. Therefore, all the parameters of P_t were set to the values of the anelastic fit in Fig. 4, with a factor multiplying the anelastic τ^{-1} as the only degree of freedom: $\tau_{\text{diel}}^{-1} = r\tau^{-1}$. It turns out that $r = 10.6$ yields a good fit. Peak P_d , appearing only in the dielectric spectrum, has an intensity $\Delta\varepsilon_d$ that clearly rises with temperature (see Fig. 3). There are two main possible causes for such a behavior: (i) P_d is due to the relaxation of a thermally excited state with energy E over the ground state, e.g., charges from a ionized defect, and therefore the relaxation strength contains the population of the ionized state as a factor, $\Delta\varepsilon_d \propto 1/\cosh(E/2T)$; and (ii) relaxation occurs between two states differing in energy by a , so that $\Delta\varepsilon_d \propto n_1 n_2 = 1/\cosh^2(a/2T)$. It is also possible that both mechanisms are present, but the data do not allow distinguishing between these possibilities, and we will consider the case $a \neq 0$, $E = 0$. Note that the two mechanisms give similar temperature dependence of $\Delta\varepsilon_d$ in a broad temperature range if $E \sim 1.5a$. The shape of P_d could be better reproduced with the Cole-Cole expression for broadening, so that the expression for fitting P_d was

$$\varepsilon_d'' = \frac{\Delta_d}{T} \frac{\sin(\pi\alpha_d/2)}{\text{sech}^2(a_d/2T) \cosh[\alpha_d \ln(\omega\tau_d)] + \cos(\pi\alpha_d/2)} \quad (5)$$

and $\tau_d = \tau_{d0} \exp(W_d/T)$. The thick curves in Fig. 6 are the resulting fit with linear backgrounds, and also P_t and P_d are shown. The parameters of P_d are $a_d = 150$ K (150 K), $\tau_{d0} = 1 \times 10^{-15}$ s (6×10^{-15} s), $W_d = 1270$ K (1270 K), and $\alpha_d = 0.26$ (0.38), where the values in parentheses are obtained from the measurements on BCY15 (data in Fig. 3). The small values of τ_{d0} are in agreement with the electronic origin of the relaxation. However, considering the extreme peak broadening (small α_d), it cannot be excluded that a correlated dynamics is present, which may be better described by a Vogel-Fulcher-type $\tau(T)$ rather than an Arrhenius one.

D. Intensity of P_t

1. Electric dipole of the OH group

The dependence of the intensity of the anelastic P_t on the H content and the marked shift to higher temperature with the heavier D isotope mass leave little doubt that anelastic P_t is due to the fast motion of H around a same O with a dynamics dominated by tunneling. It is also clear that P_t has its dielectric counterpart (Fig. 3, curves 1 and 2). A puzzling feature of the dielectric P_t is its very small intensity; therefore we discuss now the estimated strengths of dielectric and anelastic relaxations. The dielectric relaxation strength associated with various types of H jumps should be relatively

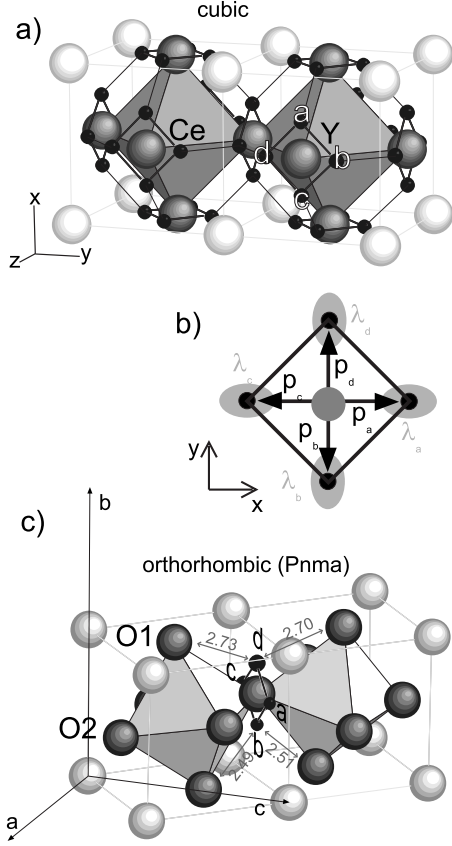


FIG. 7. (a) Network of the H sites in the cubic structure of BCY: Ba=white, O=gray; H sites =black; Y/Ce are at the centers of the octahedra. (b) Electric dipoles \mathbf{p}_i^{OH} and elastic quadrupoles λ_i^{OH} associated with the four orientations of the OH⁻ ion. (c) Distorted environment of a set of four sites around an O2 atom in the orthorhombic structure (atomic positions except H from Ref. 3 in *Pnma* setting).

easy to estimate in a medium which is not particularly highly polarizable such as BCY. Let us first consider P_Y , interpreted as the reorientation of an effective dipole Y'-OH⁻, where the Kröger-Vink notation expresses the fact that Y³⁺ has an excess $-e$ charge with respect to Ce⁴⁺ of the perfect lattice and OH⁻ has a $+e$ charge with respect to O²⁻. On the time scale of the H reorientation among different faces of the cube containing Y, the fast motion around each O is completely averaged out with the barycenter near O, thus giving rise to an effective dipole $p^Y = ea/2$, where a is the lattice constant of the cubic perovskite [Fig. 7(a)]. A jump to a different cube face will cause a change in the dielectric dipole of $\Delta p = e\sqrt{2}a$. Setting $a = 4.39$ Å, Eq. (2) gives a dielectric relaxation strength $\Delta\epsilon^Y = c_{Y-H} \times 1060$ at 300 K. Therefore the intensity $\Delta\epsilon \approx 30$ of P_Y at $x=0.15$ (Fig. 2) is obtained by setting $c_{Y-H} \approx 0.03$, namely, that at this temperature $\sim 20\%$ of H is trapped by Y. It is likely, however, that c_{Y-H} is closer to c_H but the effective dipole p^Y is reduced by the surrounding polarization and distortion. The dipole involved in P_t instead is associated with the OH ion in its four equilibrium positions [Fig. 7(b)]:

$$p_a^{\text{OH}} = -p_c^{\text{OH}} = qd\hat{x},$$

$$p_b^{\text{OH}} = -p_d^{\text{OH}} = -qd\hat{y}, \quad (6)$$

where $d \sim 1$ Å is the O-H separation. The actual charge on O and H is likely reduced by polarization effects, and it has been calculated by atomistic simulations³⁴ as $-1.426e$ and $0.426e$, thus giving $q = 0.426e$. A reorientation of the OH ion by 90° causes $\Delta p^{\text{OH}} = q\sqrt{2}d$ and, setting $E_a = 64$ K from the fit, the resulting relaxation strength of peak P_t at $T \approx 35$ K should be $\Delta\epsilon^Y = c_{Y-H} \times 41$. The result is that P_t at 35 K should be ~ 26 times smaller than P_Y at 300 K, but instead it is nearly 1000 times smaller, therefore nearly 40 times smaller than expected.

2. Elastic quadrupole of the OH group

The anelastic case is different, since the elastic quadrupole λ corresponds to the long-range component of the strain associated with the OH ion and cannot be estimated in an obvious manner as the electric dipole. It can only be said that the OH ion in the cubic configuration in Fig. 7 has orthorhombic symmetry. Therefore in an xy cube face it is

$$\lambda_a^{\text{OH}} = \lambda_c^{\text{OH}} = \begin{pmatrix} \lambda_1^{\text{OH}} & 0 & 0 \\ 0 & \lambda_2^{\text{OH}} & 0 \\ 0 & 0 & \lambda_3^{\text{OH}} \end{pmatrix} \quad (7)$$

and $\lambda_{b,d}^{\text{OH}}$ have the x and y components exchanged. The reorientation of OH by 90° causes a change $\Delta\lambda^{\text{OH}} = \|\lambda_1^{\text{OH}} - \lambda_2^{\text{OH}}\|$. On the longer time scale of relaxation P_Y , the four positions of the face $\perp z$ produce a tetragonal quadrupole,

$$\lambda^z = \begin{pmatrix} \frac{1}{2}(\lambda_1^{\text{OH}} + \lambda_2^{\text{OH}}) & 0 & 0 \\ 0 & \frac{1}{2}(\lambda_1^{\text{OH}} + \lambda_2^{\text{OH}}) & 0 \\ 0 & 0 & \lambda_3^{\text{OH}} \end{pmatrix}, \quad (8)$$

plus in the case of the Y-OH complex, a possible additional distortion,

$$\lambda^{Yz} = \begin{pmatrix} \lambda_2^Y & 0 & 0 \\ 0 & \lambda_2^Y & 0 \\ 0 & 0 & \lambda_1^Y \end{pmatrix}. \quad (9)$$

Then, the anelastic peak P_Y associated with the reorientation of the tetragonal defect complex Y-OH has $\Delta\lambda^Y = (\lambda_1^Y - \lambda_2^Y) + \lambda_3^{\text{OH}} - \frac{1}{2}(\lambda_1^{\text{OH}} + \lambda_2^{\text{OH}})$. Lacking any method for estimating these components of the elastic quadrupoles associated with OH and Y-OH complexes, we cannot exclude that $\Delta\lambda^{\text{OH}}$ is approximately ten times smaller than $\Delta\lambda^Y$, so determining a reduction in the intensity of P_t by 2 orders of magnitude with respect to P_Y . Then, the small intensity of the anelastic P_t does not necessarily constitute a problem as the dielectric intensity does.

3. Anelastic and dielectric relaxation strengths of tunneling states in a cubic environment

The explanation of why the intensity of the dielectric P_t is so much smaller than expected from a simple estimate of the

magnitude of dipole change would be easy if BCY was cubic or very close to cubic. In fact, in the case of coherent tunneling among four nearly equivalent positions, the effective dipole strength for transitions between H eigenstates would be much smaller than for hopping among the same positions, at variance with the anelastic case. The Hamiltonian of the symmetric four-level system (FLS) of H may be written in the basis $|i\rangle$, where H is localized in each site $i=a-d$ as

$$H_{\text{cub}} = \frac{1}{2} \begin{bmatrix} 0 & t & 0 & t \\ t & 0 & t & 0 \\ 0 & t & 0 & t \\ t & 0 & t & 0 \end{bmatrix}, \quad (10)$$

where t is the effective tunneling matrix element between adjacent sites dressed with the interaction with phonons and the site energies are all set to 0. The eigenstates of H_{cub} are

$$|1,4\rangle \propto \begin{bmatrix} \pm 1 \\ 1 \\ \pm 1 \\ 1 \end{bmatrix}, \quad |2\rangle \propto \begin{bmatrix} 0 \\ -1 \\ 0 \\ 1 \end{bmatrix}, \quad |3\rangle \propto \begin{bmatrix} -1 \\ 0 \\ 1 \\ 0 \end{bmatrix}. \quad (11)$$

Two states are delocalized over all sites, with energies $E_{1,4} = \mp t/2$, and two are delocalized over either pair of opposite sites, with energies $E_{2,3}=0$. The associated electric dipoles \mathbf{p}^{FLS} and elastic quadrupoles λ^{FLS} may be obtained by taking the matrix elements $\lambda_i^{\text{FLS}} = \langle i | \lambda^{\text{OH}} | i \rangle$ and $\mathbf{p}_i^{\text{FLS}} = \langle i | \mathbf{p}^{\text{OH}} | i \rangle$, with λ^{OH} and \mathbf{p}^{OH} given above. It is evident that \mathbf{p}^{OH} averaged over any of the above states is null, since opposite sites are equally occupied and cancel out the respective dipoles. Then, no dielectric relaxation is expected from H tunneling in a cubic environment, or also next to a Y dopant, which leaves the fourfold symmetry of the FLS. The elastic quadrupoles, instead, being centrosymmetric as in Eq. (7), are equal within pairs of opposite sites; and transitions between the two intermediate eigenstates cause a change in elastic quadrupole by $\Delta\lambda^{\text{OH}} = \|\lambda_1^{\text{OH}} - \lambda_2^{\text{OH}}\|$. Transitions between states 2,3 and 1,4 cause a change of $\Delta\lambda^{\text{OH}}/2$ and those between 1 and 4 cause no anelastic relaxation. Therefore, the formation of FLS with weak deviations from fourfold symmetry would explain why the dielectric relaxation from H tunneling is much more effectively suppressed than the anelastic one, with respect to classical reorientation.

A picture such as this, with H and D performing coherent tunneling within nearly symmetric FLS, has been thoroughly studied by anelastic relaxation in Nb with substitutional traps.²⁴⁻²⁷ Also in that case H tunnels within rings of four equivalent tetrahedral sites on the faces of the bcc cells with a dopant in the center and performs overbarrier jumps to the neighboring rings, which form a network exactly as in the cubic perovskite [see Fig. 7(a)]. In $\text{Nb}_{1-x}\text{Zr}_x$ single crystals with $x=0.0013$, it was also possible to distinguish well separated relaxation processes arising from transitions involving eigenstates with different symmetries, only moderately perturbed by interactions among dopants.²⁶ In addition, the dependence of the anelastic relaxation due to the slower reorientation among different cube faces on the symmetry of the

excitation stress²⁵ provides evidence that the symmetry of the FLS persists at least up to 150 K, implying that the H eigenstates maintain coherence up to that temperature. It should be noted that the measured effective tunneling matrix element between tetrahedral sites in Nb is $t \sim 0.2$ meV for H and 0.02 meV for D, corresponding to $t/k_B=2$ and 0.2 K or $t/h=4 \times 10^{10}$ and 4×10^9 s⁻¹, respectively. It appears therefore that coherence is maintained both at temperatures orders of magnitude larger than t/k_B and with tunneling frequencies on the order of phonon frequencies.

A theoretical basis for the persistence of quantum coherence at such high temperatures comes from analytical and numerical analysis of the centrosymmetric FLS, where coherent oscillations of the H populations are found even for strong interaction with the thermal bath,³⁵ and from the analysis of the dynamics of polarons using the dynamical mean-field approximation,³⁶ which is a nonperturbative approach. It is shown that the coherence of the state including tunneling particle and surrounding polaronic distortion is maintained at temperatures up to a substantial fraction of the energy of the phonon coupled with the particle, $k_B T \sim 0.2\hbar\omega_0$, and also in the case of strong coupling, where the energy for the polaron formation is $E_p > \hbar\omega_0$. We assume that $E_p \approx 1$ eV from the theoretical estimate³⁷ of the self-trapping energy of H in BaZrO_3 and that the strongest coupling is with the O-Ce-O bending mode [in BaCeO_3 $\hbar\omega_0 = 41$ meV (Ref. 38)] modulating the distance with the neighboring O atoms and therefore the hydrogen bonds with them. Then we are in the limit of strong coupling, and the dynamical mean-field analysis³⁶ ensures us that coherent states may be maintained up to $0.2\hbar\omega_0/k_B \approx 100$ K. This holds for both H and D, since the smallness of the dressed tunneling matrix element should not be a problem until the tunneling frequency is larger than the measuring frequency.

4. Tunneling states in the orthorhombic lattice

The main problem with the above explanation of the smallness of the dielectric relaxation strength of P_t is that BCY at low temperature is not cubic but orthorhombic, and the FLS should be far from symmetric. Figure 7(c) shows an undistorted ring, as in the cubic case, between two octahedra tilted as in the orthorhombic $Pnma$ low-temperature structure of $\text{BaCe}_{0.9}\text{Y}_{0.1}\text{O}_{3-\delta}$.³ The O atoms split into two types: O1 at the vertices of the octahedra along the b axis and O2 near the ac plane. Neutron diffraction indicates that at 4.2 K, H in BCY occupies a site near the one labeled d in Fig. 7(c), which is also the one with the largest distances from the next-nearest-neighbor O atoms. It is therefore reasonable to assume that in the distorted orthorhombic structure H occupies sites slightly displaced from those in the cubic cell and that the site energy is mainly determined by the mean distance \bar{l} from the two next-nearest-neighbor O atoms, with which some hydrogen bonding can take place.⁹ For the sites labeled a-d in Fig. 7(b) it is $\bar{l}=2.66, 2.71, 2.53,$ and 2.50 , respectively, so that the site energies may be written as $E_a \approx E_b = a/2$, $E_c \approx E_d = -a/2$. The Hamiltonian of the tunnel system becomes

$$H_{\text{ortho}} = \frac{1}{2} \begin{bmatrix} a & t & 0 & t \\ t & a & t & 0 \\ 0 & t & -a & t \\ t & 0 & t & -a \end{bmatrix}, \quad (12)$$

with eigenstates

$$|1,2\rangle \propto \begin{bmatrix} a - \delta \\ \mp(a - \delta) \\ \mp t \\ t \end{bmatrix}, \quad |3,4\rangle \propto \begin{bmatrix} a + \delta \\ \mp(a + \delta) \\ \mp t \\ t \end{bmatrix} \quad (13)$$

and energies $E_{1,2} = (-\delta \mp t)/2$, $E_{3,4} = (\delta \mp t)/2$, where $\delta = \sqrt{a^2 + t^2}$. This means that when $a \gg t$, there are two low-energy eigenstates with H mainly delocalized over sites c and d and two higher-energy eigenstates delocalized over sites a and b. These states have an electric dipole $p \approx ed/\sqrt{2}$ oriented roughly midway between the two occupied sites. Therefore, while in the limit $a \ll t$, valid for the cubic ideal case, the H atom is delocalized over all sites and the electric dipole is averaged out to almost zero, H in BCY at low temperature is expected to be in the opposite limit $a \gg t$, where the averaging effect of the electric dipole occurs only within the pairs ab and cd of low- and high-energy states, without a suppression of the dipole magnitude.

The present data do not allow estimation of t , neither do we know of estimates of the energy asymmetry a due to the orthorhombic distortion. However based on the comparison with the better known case of Zr-H complexes in Nb, we should be in the limit $a \gg t$. In fact, t should be smaller than in Nb, since, assuming an O-H bond $\approx 0.93 \text{ \AA}$ long, the distance between neighboring sites is $\sim 1.3 \text{ \AA}$ in BCY, while it is only 1 \AA in Nb. In addition, the maximum of the anelastic relaxation is shifted to higher temperature with respect to $\text{Nb}_{1-x}\text{Zr}_x\text{H}_y$, indicating slower transition rates. Therefore it should be $t/k_B \ll 1 \text{ K}$, the value found in Nb. On the other hand, we expect $a/k_B \gtrsim 10^2 \text{ K}$, considering that the random strains due to $< 1 \text{ at. \%}$ of impurities in Nb cause a/k_B of tens of kelvins,²⁷ and the strain associated with the octahedral tilts in orthorhombic BCY is certainly larger. Another indication that a due to the orthorhombic distortion is large comes from the theoretical estimate³⁷ $E_p \approx 1 \text{ eV}$ of the self-trapping energy of H in BaZrO_3 .

5. Symmetric tunneling states within twin walls

After these arguments, it is puzzling that the intensity of the dielectric P_d in orthorhombic BCY is so small. The situation is similar to that found in hydrated $\text{BaCe}_{1-x}\text{Nd}_x\text{O}_{3-\delta}$, where a low-temperature dielectric relaxation exists whose rate has a temperature dependence indicating tunneling. However, it was concluded that if all the protons were responsible for such a relaxation, the intensity should be 50 times larger; therefore only special defect configurations contributed to that relaxation.²⁸ In the present case, unless the OH dipole is smaller than estimated,³⁴ less than 3% of the H atoms should contribute to P_t and it should be explained what kind of particular configuration exhibits tunneling and what is the dynamics of the majority H atoms. In

fact, both neutron spectroscopy at high temperature^{7,8} and simulations⁹ indicate that the reorientation of the OH ion is much faster than the hopping between different O atoms in perovskite cerates. A possible scenario is that the fast reorientation occurs only in high-temperature phases that are cubic or less distorted than the orthorhombic phase, whereas in the latter H is nearly localized at lowest energy site, close to site d in Fig. 7(b). Then the reorientation of the OH ion would be slower than that producing P_t and might be identified with P_h or some broad peak masked by the tail of P_Y and by P_h , perhaps the one around 100 K in Fig. 1. In this scenario the tunneling motion would appear only in particularly symmetric environments, e.g., at the boundaries between different structural domains. We are not aware of any study of the density, width, and morphology of the domain boundaries in BCY. However indirect support of this mechanism comes from a simulation on orthorhombic CaTiO_3 , where the twin walls are found to be about six pseudocubic cells wide and to trap the O vacancies.³⁹ It is also proposed that the diffusion of O vacancies should be faster within the twin planes, which are more symmetric than the orthorhombic bulk. Also in the case of H in BCY, the reorientation rate of H might be faster at the twin walls, but the relevance of this effect on the long-range mobility would be limited, since the rate limiting step is not the OH reorientation but the hopping to a different O atom. We think however that the effect of the greater symmetry at the twin walls should be studied also in relation with the hopping mechanism and in the high-temperature phases of BCY. Also simulations on BaZrO_3 and CaTiO_3 suggest that the octahedral tilting is essential in determining H site energies and diffusion paths.⁴

If H tunneling in the orthorhombic phase indeed occurs only in the twin boundaries, then the intensity of peak P_t would depend on their density, which in turn may depend on microstructure and thermal history. This might be the reason why the dielectric P_t in BCY15 is nearly three times more intense than in BCY10, a feature that is otherwise difficult to explain. Additional measurements are necessary to clarify this issue.

Another factor that may contribute to lowering of the dielectric relaxation strength of P_t is the lattice polarization around the OH^- ion. In fact, the actual dipole is not the bare OH^- dipole with nominal charges ± 1 , but it is due to the OH^- complex plus the shifted surrounding atoms and with charge transfers with respect to the purely ionic case. We estimated the intensity of dielectric P_t assuming the OH dipole calculated in Ref. 34, but the actual dipole may be even smaller.

V. CONCLUSIONS

Three main relaxation processes have been identified both in the anelastic and dielectric spectra as due to hopping of H around an Y dopant (peak P_Y), hopping far from dopants (peak P_h), and tunneling within the four sites around the same O atom (peak P_t). An additional dielectric relaxation maximum around 60 K (P_d) does not involve H motion but rather appears as a relaxation of electronic origin such as small polaron hopping. Peak P_t can be fitted assuming a

relaxation rate that is Arrhenius type above ~ 50 K, possibly due to two-phonon transitions with optical phonons rather than to overbarrier hopping; exhibits a T^7 dependence typical of two-phonon transitions with acoustic phonons below 50 K; and finally becomes nearly constant below ~ 20 K, as expected from one-phonon transitions. The isotopic substitution with D decreases the rate by a factor of 8. The dielectric spectra are more difficult to analyze, due to the presence of peak P_d and possibly other peaks at lower temperature, but reasonable fits are obtained using the same anelastic expression of P_t with a rate increased by approximately ten times. Such a difference in the rate may be due to the fact that, although not clearly distinguishable, there are at least three anelastic and dielectric relaxation modes contributing to P_t , having different strengths and rates.

The intensity of the dielectric P_t is nearly 40 times smaller than expected from a simple estimate of the reorientation of the electric dipole associated with the OH^- ion. It is shown that, while this suppression of the dielectric relaxation would be easily explained in terms of coherent tunneling of

H around O in a cubic environment, the same seems not to be true in the presence of the low-temperature orthorhombic distortion. As an alternative or concomitant explanation, it is proposed that H tunneling may occur only in the more symmetric cells within twin walls, while slower semiclassical reorientation of OH^- would occur within the orthorhombic domains. In addition, the total dipole of OH^- ion and surrounding lattice polarization may be smaller than expected.

ACKNOWLEDGMENTS

We wish to thank S. Ciuchi for useful discussions on the coherence of the polaron states, O. Frasciello for valuable suggestions on the dielectric measurements, and F. Corvasce, M. Latino, and A. Morbidini for their technical assistance. This research is supported by the FISIR Project of MIUR Italy "Celle a combustibile ad elettroliti polimerici e ceramici: dimostrazione di sistemi e sviluppo di nuovi materiali."

- ¹K. D. Kreuer, *Solid State Ionics* **97**, 1 (1997).
- ²M. Glerup, F. W. Poulsen, and R. W. Berg, *Solid State Ionics* **148**, 83 (2002).
- ³K. S. Knight, *Solid State Ionics* **127**, 43 (2000).
- ⁴M. A. Gomez, M. A. Griffin, S. Jindal, K. D. Rule, and V. R. Cooper, *J. Chem. Phys.* **123**, 094703 (2005).
- ⁵W. Münch, G. Seifert, K. D. Kreuer and J. Maier, *Solid State Ionics* **86-88**, 647 (1996).
- ⁶T. Ito, T. Nagasaki, K. Iwasaki, M. Yoshino, T. Matsui, H. Fukazawa, N. Igawa, and Y. Ishii, *Solid State Ionics* **178**, 607 (2007).
- ⁷M. Pionke, T. Mono, W. Schweika, T. Springer, and H. Schober, *Solid State Ionics* **97**, 497 (1997).
- ⁸Th. Matzke, U. Stimming, Ch. Karmonik, M. Soetratmo, R. Hempelmann, and F. Güthoff, *Solid State Ionics* **86-88**, 621 (1996).
- ⁹M. E. Björketun, P. G. Sundell, and G. Wahnström, *Phys. Rev. B* **76**, 054307 (2007).
- ¹⁰R. Hempelmann, Ch. Karmonik, Th. Matzke, M. Cappadonia, U. Stimming, T. Springer, and M. A. Adams, *Solid State Ionics* **77**, 152 (1995).
- ¹¹R. Hempelmann, M. Soetratmo, O. Hartmann, and R. Wäppling, *Solid State Ionics* **107**, 269 (1998).
- ¹²F. Giannici, A. Longo, F. Deganello, A. Balerna, A. S. Arico, and A. Martorana, *Solid State Ionics* **178**, 587 (2007).
- ¹³H. Maekawa, Y. Ukei, K. Morota, N. Kashii, J. Kawamura, and T. Yamamura, *Solid State Commun.* **130**, 73 (2004).
- ¹⁴F. Deganello, G. Marci, and G. Deganello *J. Eur. Ceram. Soc.* (to be published).
- ¹⁵Q. Xu, D.-P. Huang, W. Chen, J.-H. Lee, H. Wang, and R.-Z. Yuan, *Scr. Mater.* **50**, 165 (2004).
- ¹⁶A. S. Nowick and B. S. Berry, *Anelastic Relaxation in Crystalline Solids* (Academic, New York, 1972).
- ¹⁷F. Craciun (unpublished).
- ¹⁸A. S. Nowick and W. R. Heller, *Adv. Phys.* **14**, 101 (1965).
- ¹⁹F. Cordero, *Phys. Rev. B* **47**, 7674 (1993).
- ²⁰Y. Du, *J. Phys. Chem. Solids* **55**, 1485 (1994).
- ²¹L. Zimmermann, H. G. Bohn, W. Schilling, and E. Syskakis, *Solid State Ionics* **77**, 163 (1995).
- ²²M. E. Björketun, P. G. Sundell, G. Wahnström, and D. Engberg, *Solid State Ionics* **176**, 3035 (2005).
- ²³W. Münch, K. D. Kreuer, S. T. Adams, G. Seifert, and J. Maier, *Phase Transitions* **68**, 576 (1999).
- ²⁴G. Cannelli, R. Cantelli, F. Cordero, and F. Trequattrini, *Phys. Rev. B* **49**, 15040 (1994).
- ²⁵G. Cannelli, R. Cantelli, F. Cordero, F. Trequattrini, and H. Schultz, *J. Alloys Compd.* **231**, 274 (1995).
- ²⁶F. Cordero, A. Paolone, and R. Cantelli, *J. Alloys Compd.* **330-332**, 467 (2002).
- ²⁷*Tunneling Systems in Amorphous and Crystalline Solids*, edited by P. Esquinazi (Springer, Berlin, 1998).
- ²⁸I. Kuskovsky, B. S. Lim, and A. S. Nowick, *Phys. Rev. B* **60**, R3713 (1999).
- ²⁹C. P. Flynn and A. M. Stoneham, *Phys. Rev. B* **1**, 3966 (1970).
- ³⁰M. I. Klinger, *Phys. Rep.* **94**, 183 (1983).
- ³¹V. Storchak, J. H. Brewer, W. N. Hardy, S. R. Kreitzman, and G. D. Morris, *Phys. Rev. Lett.* **72**, 3056 (1994).
- ³²In Ref. **23** the barrier is calculated assuming that the proton is a classical particle. Yet the comparison with W in Eq. (4) should be meaningful, since W is the effective activation energy of the fast H motion in the high-temperature limit, which eventually becomes overbarrier hopping.
- ³³A. Mineshige, S. Okada, M. Kobune, and T. Yazawa, *Solid State Ionics* **177**, 2443 (2006).
- ³⁴R. Glöckner, M. S. Islam, and T. Norby, *Solid State Ionics* **122**, 145 (1999).
- ³⁵M. Winterstetter and M. Grifoni, *Phys. Rev. B* **62**, 3237 (2000).
- ³⁶S. Fratini and S. Ciuchi, *Phys. Rev. Lett.* **91**, 256403 (2003).
- ³⁷P. G. Sundell, M. E. Björketun, and G. Wahnström, *Phys. Rev. B* **76**, 094301 (2007).
- ³⁸I. Charrier-Cougoulic, T. Pagnier, and G. Lucazeau, *J. Solid State Chem.* **142**, 220 (1999).
- ³⁹M. Calleja, M. T. Dove, and E. H. Salje, *J. Phys.: Condens. Matter* **15**, 2301 (2003).